Axial Dispersion Model for Simulation of an Airlift Bioreactor

I. Sikula, J. Markoš

Institute of Chemical and Environmental Engineering, Faculty of Chemical and Food Technology, Slovak University of Technology in Bratislava, Radlinského 9, 812 37 Bratislava, Slovak Republic

Abstract

The airlift reactors have potential application in biotechnology industries due to their simple construction and less shear stress imposed on shear sensitive cells compared with the mechanically stirred tanks.

This work was focused on mathematical modeling of the fermentation process in an internal loop airlift reactor (IALR). Simulation results were verified on the batch fermentation of the gluconic acid by the strain Aspergillus niger which has been chosen as a model system. The fermentation was carried out in three laboratory IALRs (each one with different scale: 12, 40 and 200 liters, respectively) and performed in growth or non-growth conditions. Model of the ILALR is based on the material balance of each compound taking a part of reaction. From the various hydrodynamic and mixing point of view the reactor was divided into four main parts: bottom, riser, separator and downcomer. Each zones of that reactor were modeled separately according to mixing properties within (ideal mixing or plug flow with axial dispersion).

Parameters of the model, such as axial dispersion coefficient, mass transfer coefficient of oxygen, gas hold-ups, and circulation velocities, were predicted using experimentally determined correlations.

The results of the simulations and experiments are in sufficient agreement.

Keywords: airlift bioreactor, gluconic acid fermentation, mathematical modeling, scale-up

1. Introduction

Bioreactors have the potential to become integrated in the development of high-value products and replace the existing chemical-based commodity processes. The most common type of aerobic bioreactor in use today, is the stirred tank reactor with baffles and agitators and other internals designed for specific applications. However, for certain industrial scale applications, pneumatically agitated airlift reactors (ALR) provide a simple design with no moving parts and generate lower shear rates for shear-sensitive microorganisms. Additionally, increased mass transfer due to enhanced oxygen solubility at higher pressures can be achieved in tall ALR

vessels. Airlift reactors are useful for aerobic processes mainly in waste water or gas treatment. In recent years a few interesting applications of ALRs appeared in the literature [1-3]. Mixing in ALRs is usually imperfect therefore models of ideal mixing or plug flow applied for the whole reactor are not recommended. In an ALR four main zones are recognized: the bottom where the gas distributor is installed and medium is recycled from the downcomer; the riser (in the case of the internal loop ALR (ILALR) it is regularly a draft tube) where the medium flows upwards; the gas separator and the downcomer. Each zone use is usually modeled separately.
The most frequently used models are based on either a cascade of ideally mixed tanks (CSTRs) [4-7] or plug flow models with axial dispersion (ADM) [1, 2, 8]. In the first model non-ideal mixing is described by the number of tanks which is different in each zone. The second one incorporates the non-ideality of mixing in the coefficient of axial dispersion for the relevant zone (riser, downcomer). For a successful simulation the reactor geometry and the proper kinetic and hydrodynamic parameters of the modeled device are needed. In case of an aerated system it is important to know the reliable mass transfer parameters because the rate of the inter-phase mass transfer is often the limiting step in the process.
In this work the plug flow model with axial dispersion was applied on ILALR modeling. The capability of this model was tested for process simulations. The simulation results were verified by experimental data obtained in an 40 dm^3 and 200 dm^3 ALR. The reaction system was based on aerobic oxidation of glucose to gluconic acid in the presence of a fungal strain *Aspergillus niger* which is characterized by high activity of glucose oxidase (E) and catalase (CAT) [1]. This system is considered as a two-phase one containing a gas and a pseudo-homogenous liquid-solid phase.

2. Theoretical

In the mathematical model of ILALR, four parts of the reactor interconnected and modeled separately are involved (see Fig. 1).

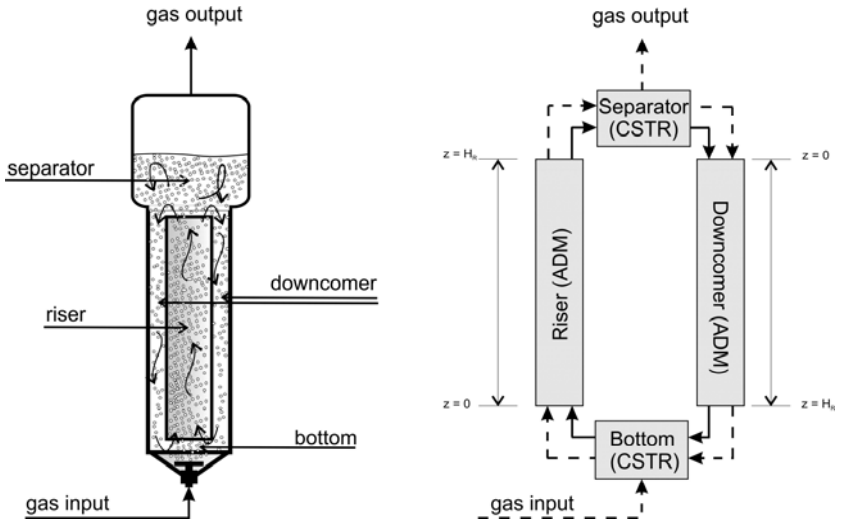

Fig. 1: Schematic diagram of the mixing model of an ILALR (liquid flow – full lines, gas flow – dashed lines).

It is expected that the bottom part and separator behave as ideally mixed compartments respectively. Modeling of non-ideal mixing in the riser and the downcomer is presented by plug flow with axial dispersion. Since the process is isothermally controlled, only the material balance is needed. Material balances for oxygen (i = O) in the separate sections of the reactor can be written as follows:

Bottom
gas phase

$$V_{\mathrm{B}}\varepsilon_{\mathrm{GR}}\frac{dc_{i,\mathrm{B}}^{\mathrm{G}}}{dt}=\left(\dot{V}_{\mathrm{D}}^{\mathrm{G}}c_{i,\mathrm{D}}^{\mathrm{G}}\right)_{z=H_{\mathrm{R}}}-(1-\varepsilon_{\mathrm{GR}})V_{\mathrm{B}}k_{\mathrm{L}}a_{\mathrm{R}}\left(c_{i,\mathrm{B}}^{*\mathrm{L}}-c_{i,\mathrm{B}}^{\mathrm{L}}\right)-\dot{V}_{\mathrm{B}}^{\mathrm{G}}c_{i,\mathrm{B}}^{\mathrm{G}}+\dot{V}_{\mathrm{in}}^{\mathrm{G}}c_{i,\mathrm{in}}^{\mathrm{G}} \qquad (1)$$

liquid phase

$$V_{\mathrm{B}}\left(1-\varepsilon_{\mathrm{GR}}\right)\frac{dc_{i,\mathrm{B}}^{\mathrm{L}}}{dt}=\dot{V}_{\mathrm{D}}^{\mathrm{L}}c_{i,\mathrm{D}}^{\mathrm{L}}+\left(1-\varepsilon_{\mathrm{GR}}\right)V_{\mathrm{B}}k_{\mathrm{L}}a_{\mathrm{R}}\left(c_{i,\mathrm{B}}^{*\mathrm{L}}-c_{i,\mathrm{B}}^{\mathrm{L}}\right)-\dot{V}_{\mathrm{B}}^{\mathrm{L}}c_{i,\mathrm{B}}^{\mathrm{L}}+V_{\mathrm{B}}\left(1-\varepsilon_{\mathrm{GR}}\right)r_{i,\mathrm{B}} \qquad (2)$$

Separator
gas phase

$$V_{\mathrm{T}}\varepsilon_{\mathrm{GR}}\frac{dc_{i,\mathrm{T}}^{\mathrm{G}}}{dt}=\left(\dot{V}_{\mathrm{R}}^{\mathrm{G}}c_{i,\mathrm{R}}^{\mathrm{G}}\right)_{z=H_{\mathrm{R}}}-(1-\varepsilon_{\mathrm{GR}})V_{\mathrm{T}}k_{\mathrm{L}}a_{\mathrm{R}}\left(c_{i,\mathrm{T}}^{*\mathrm{L}}-c_{i,\mathrm{T}}^{\mathrm{L}}\right)-\dot{V}_{\mathrm{T}}^{\mathrm{G}}c_{i,\mathrm{T}}^{\mathrm{G}}-\dot{V}_{\mathrm{out}}^{\mathrm{G}}c_{i,\mathrm{out}}^{\mathrm{G}} \qquad (3)$$

liquid phase

$$V_{\mathrm{T}}\left(1-\varepsilon_{\mathrm{GR}}\right)\frac{dc_{i,\mathrm{T}}^{\mathrm{L}}}{dt}=\dot{V}_{\mathrm{R}}^{\mathrm{L}}c_{i,\mathrm{R}}^{\mathrm{L}}+(1-\varepsilon_{\mathrm{GR}})V_{\mathrm{T}}k_{\mathrm{L}}a_{\mathrm{R}}\left(c_{i,\mathrm{T}}^{*\mathrm{L}}-c_{i,\mathrm{T}}^{\mathrm{L}}\right)-\dot{V}_{\mathrm{T}}^{\mathrm{L}}c_{i,\mathrm{T}}^{\mathrm{L}}+V_{\mathrm{T}}\left(1-\varepsilon_{\mathrm{GR}}\right)r_{i,\mathrm{T}} \qquad (4)$$

Riser (Downcomer)
gas phase

$$\varepsilon_{\mathrm{GR(D)}}\frac{\partial c_i^{\mathrm{G}}}{\partial t}=\varepsilon_{\mathrm{GR(D)}}D_{\mathrm{aGR(D)}}\frac{\partial^2 c_i^{\mathrm{G}}}{\partial z^2}-\frac{\partial\left(U_{\mathrm{GR(D)}}c_i^{\mathrm{G}}\right)}{\partial z}-\left(1-\varepsilon_{\mathrm{GR(D)}}\right)k_{\mathrm{L}}a_{\mathrm{R(D)}}\left(c_i^{*\mathrm{L}}-c_i^{\mathrm{L}}\right) \qquad (5)$$

liquid phase

$$\left(1-\varepsilon_{\mathrm{GR\,(D)}}\right)\frac{\partial c_i^{\mathrm{L}}}{\partial t}=\left(1-\varepsilon_{\mathrm{GR\,(D)}}\right)D_{\mathrm{a\,L\,R\,(D)}}\frac{\partial^2 c_i^{\mathrm{L}}}{\partial z^2}-\frac{\partial\left(U_{\mathrm{LR\,(D)}}c_i^{\mathrm{L}}\right)}{\partial z}+ \qquad (6)$$
$$+\left(1-\varepsilon_{\mathrm{GR\,(D)}}\right)k_{\mathrm{L}}a_{\mathrm{R\,(D)}}\left(c_i^{*\mathrm{L}}-c_i^{\mathrm{L}}\right)+\left(1-\varepsilon_{\mathrm{GR\,(D)}}\right)r_i$$

The material balances for glucose, gluconic acid and biomass can be derived from Eqs.(2), (4) and (6) by substituting index *i* (*i* = S, P, X). The term of the interfacial mass transfer rate is eliminated in these equations because only oxygen participates in the mass transfer.
Initial conditions for the concentration of each compound are:

Bottom (Separator)

$$t=0:\quad c_i^{\mathrm{L}}=c_{i,\mathrm{B(T)}}^{\mathrm{L0}}\quad c_i^{\mathrm{G}}=c_{i,\mathrm{B(T)}}^{\mathrm{G0}} \qquad (7)$$

Riser (Downcomer)

$$t=0, z\in\langle 0,H_{\mathrm{R}}\rangle:\quad c_i^{\mathrm{L}}=c_{i,\mathrm{R(D)}}^{\mathrm{L0}}\quad c_i^{\mathrm{G}}=c_{i,\mathrm{R(D)}}^{\mathrm{G0}} \qquad (8)$$

Boundary conditions for Eqs. (5) and (6) are defined by following relations:

Riser (Downcomer)

$$t > 0, z = 0 \qquad c_i^{\mathrm{L}} = c_{i,\mathrm{B(T)}}^{\mathrm{L}} \qquad c_i^{\mathrm{G}} U_{\mathrm{GR(D)}} = \frac{\dot{V}_{\mathrm{B(T)}}^{\mathrm{G}}}{A_{\mathrm{R(D)}}} c_{i,\mathrm{B(T)}}^{\mathrm{G}}$$

$$t > 0, z = H_{\mathrm{R}} \qquad c_i^{\mathrm{L}} = c_{i,\mathrm{T(B)}}^{\mathrm{L}} \qquad c_i^{\mathrm{G}} U_{\mathrm{GR(D)}} = \frac{\dot{V}_{\mathrm{T(B)}}^{\mathrm{G}}}{A_{\mathrm{R(D)}}} c_{i,\mathrm{T(B)}}^{\mathrm{G}} \qquad (9)$$

When deriving the model equations, the effect of hydrostatic pressure profile along the ALR on gas phase volumetric flows (superficial velocities) and dissolved oxygen solubility were assumed. Liquid phase was assumed to be incompressible. If we assume the ideal behavior of the gas phase, the molar fraction of oxygen using results of Eqs. (1), (3) and (6) could be calculated by the following expression

$$Y_{\mathrm{O}} = \frac{c_{\mathrm{O}}^{\mathrm{G}} RT}{p} \qquad (10)$$

where p is a function of the medium level above the section defined as

$$p = p_0 + \rho_{\mathrm{L}} (1 - \varepsilon_{\mathrm{GC}}) g H_{\mathrm{L}} \qquad (11)$$

p_0 is the pressure above the liquid level at the top of the ALR, H_L is the distance between the liquid level in the separator and the actual axial position in the reactor.
In the calculation of the saturation concentration of dissolved oxygen the effect of non – volatile compounds on oxygen solubility presented in the liquid medium was taken into account using correlations available in the literature [2, 3].

Biotransformation of glucose to gluconic acid by the filamentous fungi *Aspergillus niger* represents a simple dehydrogenation reaction without involvement of complex metabolic cell pathways [4]. The overall reaction of biotransformation can be written as follows:

$$\mathrm{S} + 1/2\,\mathrm{O_2} \xrightarrow[\mathrm{CAT}]{\mathrm{E}} \mathrm{P} \qquad (\mathrm{A})$$

In the literature are presented publications where the mechanism of the catalytic glucose oxidation reaction was studied [5-7]. Gibson et al. [6] suggested the enzymatic reaction of glucose to gluconic acid to be composed of four steps. According to the mentioned mechanism the rate of product formation is described by Eq. (12):

$$r_{\mathrm{P}} = \frac{V'_{\mathrm{m}} c_{\mathrm{E}}}{\left(1 + \frac{K'_{\mathrm{PS}}}{c_{\mathrm{S}}} + \frac{K'_{\mathrm{PO}}}{c_{\mathrm{O}}^{\mathrm{L}}}\right)} \qquad (12)$$

The similar approach can be applied for *Aspergillus niger*, if we consider linear relation between the dry weight concentration of biomass and its glucose-oxidase content. The Eq. (12) can be consequently rewritten as follows:

$$r_{\mathrm{P}} = \frac{V_{\mathrm{m}} c_{\mathrm{X}}}{\left(1 + \frac{K_{\mathrm{PS}}}{c_{\mathrm{S}}} + \frac{K_{\mathrm{PO}}}{c_{\mathrm{O}}^{\mathrm{L}}}\right)} \qquad (13)$$

In growth conditions where all the compounds (substrates, minerals, proteins) necessary for the biomass growth are presented in the medium the growth rate can be described as follows:

$$r_{\mathrm{P}} = \mu_{\mathrm{m}} \frac{c_{\mathrm{S}}}{\left(K_{\mathrm{XS}} c_{\mathrm{X}} + c_{\mathrm{S}}\right)} \frac{c_{\mathrm{O}}^{\mathrm{L}}}{\left(K_{\mathrm{XO}} c_{\mathrm{X}} + c_{\mathrm{O}}^{\mathrm{L}}\right)} c_{\mathrm{X}} \qquad (14)$$

Eqs. (15) and (16) describe the rates of consumption of each substrate – glucose and dissolved oxygen:

$$r_{\mathrm{S}} = -\alpha\, r_{\mathrm{X}} - \beta\, r_{\mathrm{P}} \qquad (15)$$

$$r_{\mathrm{O}} = -\gamma\, r_{\mathrm{X}} - \delta\, r_{\mathrm{P}} \qquad (16)$$

Coefficients α and γ correspond to the contribution to glucose and oxygen consumption by growth respectively. Symbols β and δ represent the respective coefficients for glucose and oxygen, derived from the stoichiometry according to reaction (A). Kinetic parameters estimated in previous study in 12 dm^3 ILALR [8] are shown in Table 1.

Table 1: Estimated kinetic parameters

μ_{m} (h^{-1})	K_{XS} (-)	$K_{\mathrm{XO}}\times10^4$ (-)	V_{m} (h^{-1})	K_{PS} (g dm^{-3})	$K_{\mathrm{PO}}\times10^3$ (g dm^{-3})	α (-)	β (-)	γ (-)	δ (-)
0.087	5.8	1.5	2.6	1.3	2.8	2.4	0.92	0.62	0.082

In non-growth conditions only the glucose and the dissolved oxygen as substrates are presented in the medium. Thus the rate of biomass production r_{X} is equal to zero and the substrates consumption rates r_{S} and r_{O} (Eqs. (15) and (16)) both depend only on the rate of gluconic acid production.

The values of $\dot{V}^{\mathrm{G(L)}}$ and $U_{\mathrm{G(L)}}$ in Eqs. (1)-(6) and (9) represent the respective volumetric flow and superficial velocity of gas or liquid, throughout the individual sections of the ALR. As the liquid medium is a batch, the corresponding volumetric flow is constant for whole reactor and can be predicted as follows:

$$\dot{V}_{\mathrm{B(T)}}^{\mathrm{L}} = U_{\mathrm{LD}} A_{\mathrm{D}} = U_{\mathrm{LR}} A_{\mathrm{R}} \qquad (17)$$

$$U_{\mathrm{LD}} = \left(1 - \varepsilon_{\mathrm{GD}}\right) v_{\mathrm{LD}} \qquad (18)$$

where the linear velocity v_{LD} for the 40 dm^3 and 200 dm^3 ALR is obtained from our experimental measurements in two- or three-phase systems [9, 10].
Gas hold-ups $\varepsilon_{\mathrm{GR}}$, $\varepsilon_{\mathrm{GD}}$ were calculated using Eqs. (19) and (20) given below and the graphical dependence of the value α as a function of U_{GC} was presented in a previous work [10].

$$\varepsilon_{\mathrm{G}} = \frac{\left(V - V_{\mathrm{D}}\right)\varepsilon_{\mathrm{GR}} + V_{\mathrm{D}}\,\varepsilon_{\mathrm{GD}}}{V} \qquad (19)$$

$$\frac{\varepsilon_{\mathrm{GD}}}{\varepsilon_{\mathrm{GR}}} = \alpha \qquad (20)$$

The effect of the mass transfer on the gas phase volumetric flow is in this case practically negligible, because of its relatively low residence time in the reactor. Thus only the change due to the hydrostatic pressure is taken into account. Depending on the circulation regime in an ALR, different amounts of the gas are entrained into the downcomer, which is estimated by defining the mean recirculation ratio:

$$I_{rec} = \left(\frac{\varepsilon_{GD} A_D \left(v_{LD} - v_{Gs} \right)}{\dot{V}_{in}^{G}} \right)_m \qquad (21)$$

where the numerator stands for the mean gas flow rate to the downcomer and is deduced according to the classifications of the flow regimes given by Heijnen et al. [11] and the observations reported by Blažej et al. [10] for the same ALR geometry, v_{Gs} is the bubble swarm velocity of the air bubbles escaping from the liquid.

In Eqs. (5) and (6), axial dispersion coefficients are presented. In the gas phase, plug flow was expected in the riser and downcomer ($D_a = 0$). Many authors present some correlations for estimation of the liquid phase axial dispersion coefficients or corresponding Peclét numbers that were estimated on bubble columns [12-14]. Almost all these correlations predict the axial dispersion coefficient with an accuracy of ± 50%, but some authors [15-17] measured about three fold higher values under the same conditions. Hereat, the axial dispersion coefficient in the liquid phase for riser and downcomer section was determined from the Peclét numbers (see Eq.(22)) which were estimated from the experimental measurement.

$$Pe_L = \frac{H_R v_L}{D_{aL}} \qquad (22)$$

The expression H_R in Eq.(22) is the length of reactor section (riser or downcomer) and v_L means the average linear velocity of the liquid in that section.

The mass transfer coefficient values were calculated from the correlation reported by Juraščík et al. [18] resulting from the study of mass transfer in the same ILALR geometry using the dynamic pressure method.

$$k_L a_{R(D)} = K(\varepsilon_{GR(D)})^{1.2} \qquad (23)$$

Where K-value is 0.47, 0.52 and 0.54 for 12 dm^3, 40 dm^3 and 200 dm^3 ILALR respectively.

The Eqs. (1) - (6) with adequate boundary and initial conditions used to describe the behavior of an ALR present a system of ordinary differential and partial differential equations of the second order. The system of partial differential equations was converted to a set of ordinary differential equations using the finite difference method for the space coordinate. All simulations were performed in commercial software MATLAB using the ODE15s solving routine.

3. Experimental

The basic geometric parameters of an 40 dm^3 ILALR can be seen in Table 2.

Table 2 Geometrical details of the reactor used.

Working volume (dm^3)	D_C (m)	$H_{L,tot}$ (m)	H_R (m)	D_R (m)	D_{top} (m)	H_B (m)	A_D/A_R (-)	H_L/D_C (-)
12	0.108	1.34	1.145	0.070	0.157	0.030	1.23	12.4
40	0.157	1.93	1.710	0.106	0.294	0.046	0.95	12.3
200	0.294	3.10	2.700	0.200	0.294	0.061	1.01	10.5

The measurement technique and the data acquisition are explained in more detail in [4, 19]. The experiment was performed at a constant temperature (30 ± 0.3°C). Both, the oxygen probe (InPro 6800, Mettler Toledo) and the pH sensor (405-DPAS-SC-K8S, Mettler Toledo) were placed at the bottom of the downcomer [4]. The value of pH was held at the level of 5.5 ± 0.2 by titration of an NaOH solution. A 12 mol L^{-1} solution of NaOH was used in experiments carried out in the 40 dm^3 and 200 dm^3 ALR. Data acquisition of all process parameters (pH, DO, inlet pressure and temperature of gas, process temperature and the amount of NaOH added) was done by an A/D converter (API, Slovakia) connected to a PC.

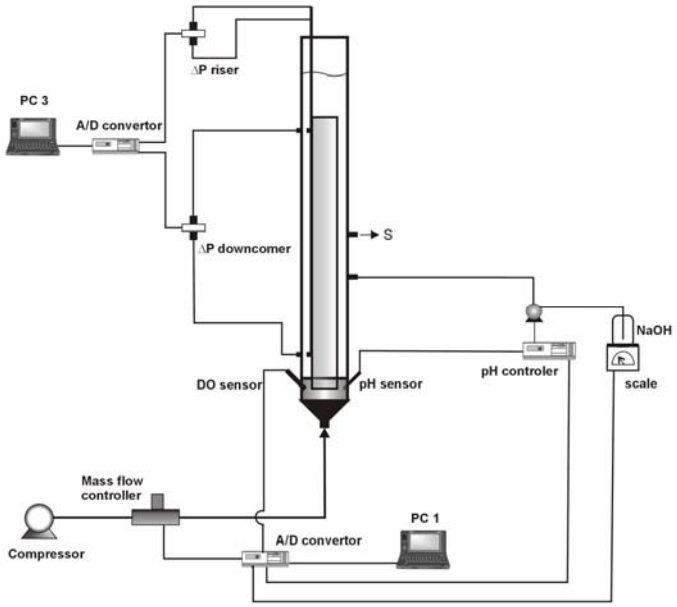

Fig. 2: Scheme of the experimental apparatus.

The microorganism Aspergillus niger CCM 8004 [1] with a high activity of glucose oxidase and catalase was used in this study. The mycelium grew in a pellet form. The inoculum was prepared in shaked flasks for 48 h. Growth conditioned fermentation was inoculated with 2 % of the working volume. A synthetic medium with a following content in g dm^{-3} was used: glucose 150, $(NH_4)_2SO_4$ 0.59, KCl 0.25, KH_2PO_4 0.25, $MgSO_4$.$7H_2O$ 0.25, $Ca(NO_3).H_2O$ 1.0, and 1.5 cm^3 dm^{-3} of 50% corn-steep liquor. The gluconic acid concentration was calculated from the actual amount of NaOH necessary for its neutralization [4]. Glucose concentration was determined by HPLC analysis. Foam level was controlled by adding the antifoam agent Lukosan (LZK, Czech Republic) in growth fermentation. The liquid mixing in the 40 dm^3 ALR was determined in the tap water – air system from the response to the salt tracer pulse (KCL, 0.005 dm^3). The conductivity data were measured using a conductivity probe with a conductometer connected to the PC. The conductivity probe was placed in the bottom part of the riser 0.07 m from the point of the tracer injection. Measurement of the liquid mixing in the geometrically similar 200 dm^3 ALR is now in state of developing. Thus these parameters were taken from a set of the experimental data for the 40 dm^3 reactor at the same hydrodynamic conditions (U_{GC}), which correspond to those in 200 dm^3 reactor. We suppose that this approach could be adequate rather than to use correlations available in literature (see previous chapter).

4. Results and Discussion

For the purpose of verification the simulation results were compared with experimental data obtained in an 40 dm^3 ALR. In this case effect of the aeration on the gluconic acid production was studied at various input volumetric flows ranging from 1200 $dm^3\ h^{-1}$ to 2400 $dm^3\ h^{-1}$(T_r = 273.15 K, p_r = 101325 Pa) (see Table 3).

Table 3: Sequence in aeration conditions during experiment in an 40 dm^3 ALR.

Experiment No.	Start(End) time (h)	$\dot{V}^G_{in\ r}$ ($dm^3\ h^{-1}$)
1.	0	1200
2.	1.13	2400
3.	3.07	1800
4.	4.56 (6.05)	1200

Trends of the parameters Pe_L in riser and downcomer section and I_{rec} incorporated in the model were estimated and are shown in Fig. 3. The dependence of the Peclet number in the downcomer section on the gas superficial velocity slightly increases, however in the riser section it is practically constant. According to our observations and estimated values of I_{rec} the reactor is in the third circulation regime with a fully developed recirculation of the gas phase. At the maximum gas flow rates approx. 22 % of the input gas is entrained into the downcomer. It is one of the important parameters that influence the supply of oxygen to the liquid phase in the downcomer. As it is shown in Fig. 4 the aeration has an important impact on the gluconic acid production since it influences the oxygen mass transfer and the dissolved oxygen level in the medium positively.

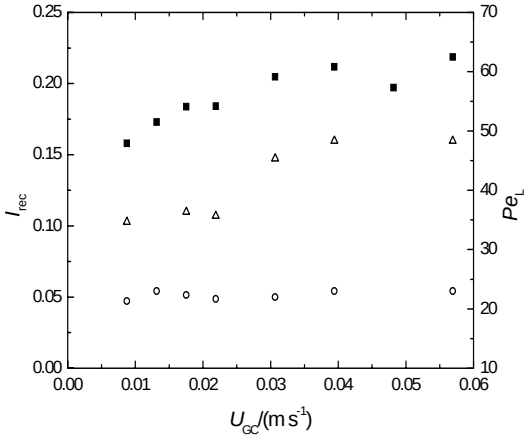

Fig. 3: Effect of the gas flow rate on the mean recirculation of gas to the downcomer (squares) and the local Peclét numbers for the liquid phase in riser (circles) and downcomer (triangles) including the range of operation conditions in an 40 dm^3 ALR.

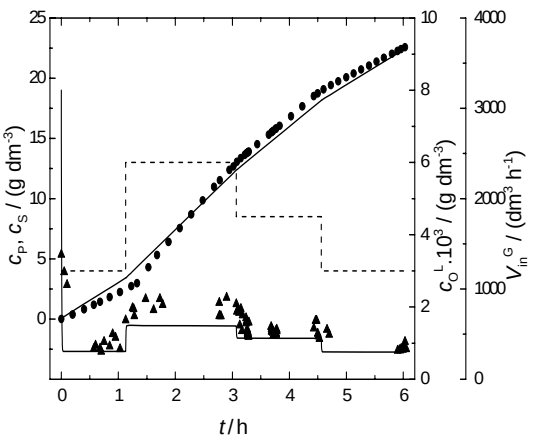

Fig. 4: Model vs. experimental data in an 40 dm^3 ALR : c_E = 5.1 g dm^{-3}, c_S (squares), c_P (circles), c_O (triangles), modeled data (solid line), input airflow $\dot{V}^G_{in\ r}$ – (dashed line).

The model data correlate with those experimental ones sufficiently and only a small deviation occurs due to the offset in the gas hold-up measurement. This discrepancy may be more obvious in long-lasting processes. In Fig. 5 dissolved oxygen profiles along the reactor are presented and the arrow shows the trend as the gas flow rate is rising.

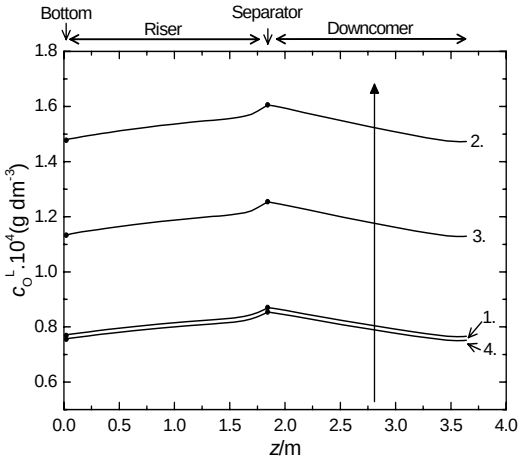

Fig. 5: Dissolved oxygen concentration profiles along the circulation loop in an 40 dm^3 ALR with respect to the aeration rate (line label – No. of experiment according Table 3). Each profile corresponds to the time close before the change into the following aeration rate.

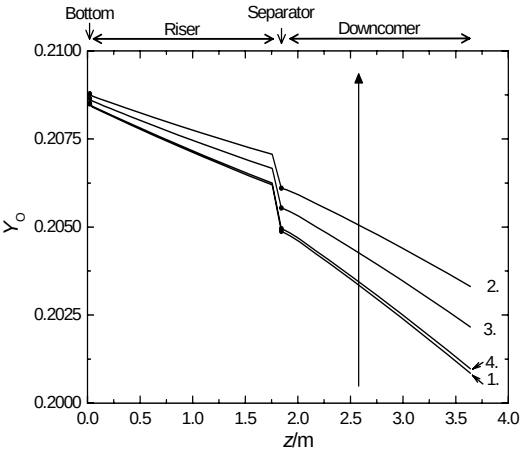

Fig. 6: The oxygen molar fraction profiles along the circulation loop in an 40 dm^3 ALR with respect to the aeration rate (line label – experiment No.) Each profile corresponds to the time close before the change into the following aeration rate.

In the first part of each profile corresponding to the riser section the liquid phase is enhanced by oxygen and the maximum value is reached in the separator section. By contrast, in the downcomer descending trend was observed. The maximum value of dissolved oxygen does not vary in its position in the reactor as the aeration conditions change. The small difference between the dissolved oxygen profiles marked by No. 1. and 4. (see Fig. 5) conditioned at the same value of volumetric gas flow input is caused by the change in the composition of non-volatile compounds (glucose, gluconic acid, Na^+ ions) in the liquid medium due to the reaction that leads to the change in the oxygen solubility. The simulation in Fig. 6 shows the oxygen molar fraction in the gas phase as a function of position in the 40 dm^3 ALR. The line parameter stands for the experiment number. The change in molar fraction is significant, mainly in the downcomer section and depends on the actual volumetric mass transfer coefficient, the volumetric flows in this part of the ALR and the mean gas recirculation ratio. Generally, it could be said that the slope of the oxygen molar fraction profile in the gas phase in the downcomer increases with the increasing aeration rate.

Fig. 7 shows the growth fermentation in the 200 dm^3 ALR. Initial and process conditions of the growth conditioned experiment a reported in Table 4.

Table 4: Initial and process conditions for 200 dm^3 ALR

Growth fermentation experiment					
V	$\dot{V}_{\text{in r}}^{\text{G}}$	c_{X}	c_{S}	c_{P}	$c_{\text{O}}^{\text{L}} \times 10^3$
(dm^3)	(dm^3 h^{-1})	(g dm^3)	(g dm^3)	(g dm^3)	(g dm^3)
200	6000	0.30	150	0	8.08

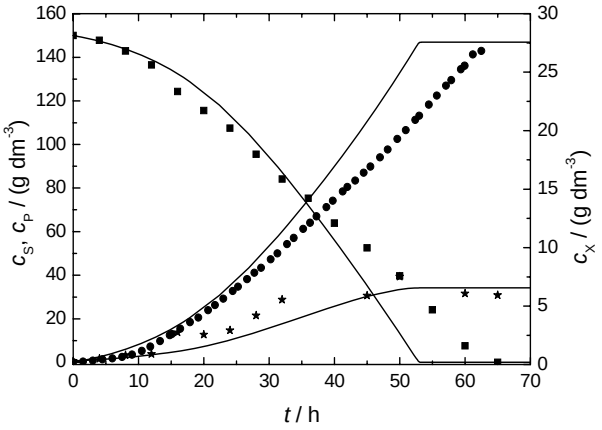

Fig. 7: Model vs. experimental data measured in the 200 dm^3 ILALR ($\dot{V}^{G}_{in\ r}$ = 6000 dm^3 h^{-1}): c_X (stars), c_S (squares), c_P (circles), modeled data (solid line) .

The accuracy of prediction of the fermentation time is around ±10 h, i.e. approx. ±15 % what is acceptable. These deviations can be caused by some factors, mainly by the inaccuracy of the measurement of the initial concentration of biomass and intensity antifoam addition (the influence of the interface oxygen transfer). It should be reminded that the accuracy of determination of the initial biomass concentration varies between ±20 %. This is caused by the character of the inoculum (biomass morphology – pellets or filaments) added to the reactor at the beginning of fermentation.
Generally, the application of the presented model could be suitable for industrial applications, particularly for process design, for finding optimal operation conditions and scale-up.

Acknowledgements: This work was supported by the Slovak Scientific Grand Agency, grant VEGA 1/3573/06.

Symbols

A	cross sectional area	m^2
c	concentration	g dm^{-3}
D	diameter	m
D_a	axial dispersion coefficient	m^2 s^{-1}
I_{rec}	recirculation ratio	-
g	gravitation acceleration	m s^{-2}
H	height	m
k_La	volumetric mass transfer coefficient	s^{-1}
K_O	oxygen saturation constant	g dm^{-3}
K_S	glucose saturation constant	g dm^{-3}
p	pressure	Pa
p_0	pressure at the top of the ALR	Pa
Pe	Peclet number	-
r_O	oxygen uptake rate	g dm^{-3} h^{-1}
r_S	substrate consumption rate	g dm^{-3} h^{-1}
r_P	product production rate	g dm^{-3} h^{-1}
r_X	biomass production rate	g dm^{-3} h^{-1}
R	gas constant	J mol^{-1} K^{-1}
t	time	h
T	temperature	K
U	superficial velocity	m s^{-1}
v	linear velocity	m s^{-1}
V	volume	m^3
$\dot{V}$	volumetric flow	m^3 s^{-1}
V_m	maximum specific production rate of the product	h^{-1}
v_{Gs}	bubble swarm velocity	m s^{-1}
Y	molar fraction	-
z	axial distance	m

Greek Letters

α	ratio of gas hold-ups in the riser and the downcomer	-
β	glucose consumption coefficient	-
δ	oxygen consumption coefficient	-
ε	hold-up	-
μ_m	maximum specific growth rate	h^{-1}
ρ	density	kg m^{-3}

Subscripts

B	bottom section
C	column
D	downcomer
E	glucose-oxidase
G	gas
i	compound (*S*, *O*, *P*)
in	incoming
L	liquid
m	mean
O	oxygen
out	outgoing
P	product
r	reference point (T_r = 273.15 K, p_r = 101325 Pa)
R	riser
S	substrate
T	separator
tot	total

Superscripts

G	gas
*	equilibrium
L	liquid
0	initial

Abbreviations

ADM	axial dispersion model
CAT	catalase
E	glucose-oxidase
DO	dissolved oxygen
CSTR	continuously stirred tank reactor

References

1. Rosenberg, M., Šturdík, E., Gömöry, J., Stanek, S., Kacina, R., and Škárka, B., *Microorganism strain Aspergillus niger CCM 8004*. 1988: Czechoslovakia. p. p. 5.
2. Rischbieter, E., Schumpe, A., and Wunder, V., *J. Chem. Eng. Data*. 41, 809 (1996).
3. Schumpe, A., *Chem. Eng. Sci.* 48, 153 (1993).
4. Klein, J., Rosenberg, M., Markoš, J., Dolgoš, O., Krošlák, M., and Krištofíková, Ľ., *Biochem. Eng. J.* 10, 197 (2002).
5. Nakamura, T. and Yasuyuki, O., *J. Biochem.* 52, 214 (1962).
6. Gibson, Q. H., Swoboda, B. E. P., and Massey, V., *J. Biol. Chem.* 239, 3927 (1964).
7. Duke, F. R., Weibel, M., Page, D. S., Bulgrin, V. G., and Luthy, J., *J. Am. Chem. Soc.* 91, 3904 (1969).
8. Sikula, I., Jurascik, M., and Markos, J., *Chem. Eng. Sci.* In Press, Corrected Proof.
9. Juraščík, M., Hucík, M., Sikula, I., Annus, J., and Markoš, J., *Chem. Pap.* 60, 441 (2006).
10. Blažej, M., Kiša, M., and Markoš, J., *Chem. Eng. Process.* 43, 1519 (2004).
11. Heijnen, J. J. and Van't Riet, K., *Chem. Eng. J.* 28, 21 (1984).
12. Deckwer, W. D., Burckhart, R., and Zoll, G., *Chem. Eng. Sci.* 29, 2177 (1974).
13. Deckwer, W. D. and Schumpe, A., *Chem. Eng. Sci.* 48, 889 (1993).
14. Towell, G. D. and Ackerman, G. H., in *Proceedings of 5th European and 2nd International Symposium on Chemical Reactor Engineering* 1977.
15. Rubio, F. C., Garcia, J. L., Molina, E., and Chisti, Y., *Chem. Eng. J.* 84, 43 (2001).
16. Rubio, F. C., Fernández, F. G. A., Sánchez Pérez, J. A., Camacho, F. G., and Molina, E., *Biotechnol. Bioeng.* 62, 71 (1999).
17. Reith, T., Renken, S., and Israel, B. A., *Chem. Eng. Sci.* 23, 619 (1968).
18. Juraščík, M., Blažej, M., Annus, J., and Markoš, J., *Chem. Eng. J.* 125, 81 (2006).
19. Blažej, M., Juraščík, M., Annus, J., and Markoš, J., *J. Chem. Technol. Biotechnol.* 79, 1405 (2004).